ORIGINAL ARTICLE

Petrophysical analysis of well logs and core samples for reservoir evaluation: a case study of southern Issaran Field, Gulf of Suez province, Egypt

Emad A. Abd El Aziz[1] · Mohamed M. Gomaa[2]

Abstract

Understanding basic petrophysical properties may enhance the recovery of residual oil saturation and help in reservoir management. Reservoir oil saturation is the fraction of the porosity of a zone occupied by oil. The trapping may increase with the increase of porosity. Oil reservoirs represent a significant fraction of the reservoirs in the world-wide. We try to make a reservoir evaluation using petrophysical analysis of well logs and core samples at Issaran Field, South Gharib Formation, West of the Gulf of Suez, southeast Egypt. This area was heavily influenced by the structural setting of the Gulf of Suez's central province, which is characterized by major SW dipping faults with a regional stratigraphic dip toward the NE. The high structural blocks are located in the center of the research area, and the low structural region is located in the southwest. South Gharib Formation is primarily composed of carbonates with few sulfates that grade upwards into sulfate-rich beds in the upper part. Laminated dolomitic limestone, with evaporites grades, changes downward into laminated dolomitic limestone and marly limestone, in the lower part. The anhydrite and dolomite units near the bottom have spotty oil stains. The structural setup is continued by the spread and deposition of this formation. We try to make analytical examination, of some reservoirs, accomplished by analyzing both well log data and core rock samples, vertically and laterally. According to the study of the horizontal permeability to vertical permeability ratio (Permeability anisotropy; λ_k), the reservoir is laminated rock ($\lambda_k = 1.1 - 5$), with a few data samples nearly isotropic ($\lambda_k = 1/1.1–1.1$) and fractured ($\lambda_k = 1/2.5–1/1.1$). Reservoir data histograms show that the most typical values of the data are 20–30% oil saturation and 7–10% porosity. The net-pay zone varies from four to 71 feet at different depths (897–1414 feet). Due to low shale content, water saturation, high effective porosity values, hydrocarbon saturation, may show higher net-pay thickness. These results may help to enhance the oil recovery. The area in the middle of the research area is suggested for future hydrocarbon development and using more petrophysical analysis.

Keywords South Gharib reservoir · Petrophysical characterization · Hydrocarbon saturation · Shale content · Isoparametric maps · Gulf of Suez

Introduction

Heterogeneous, limestone and dolomite reservoirs, deposited in shallow-shelf environments, represent a significant fraction of the reservoirs in the world-wide. Basic petrophysical properties (porosity, permeability, oil saturation, pressure, and relative permeability) vary horizontally and vertically. Understanding these basic petrophysical properties change with rock lithology and can enhance recovery of residual oil saturation and help in reservoir management. The research oil field is present in the southeastern section of the Issaran Field, along the western bank of the Gulf of Suez, and is limited by longitudes 32 44′ 30.94"–32 45′ 59.26" E., and

✉ Emad A. Abd El Aziz
  Emadnrc2002@yahoo.com

  Mohamed M. Gomaa
  mmmsgomaa@yahoo.com

[1] Geophysical Sciences Department, National Research Centre, El-Behoos St., Dokki, Cairo, Egypt

[2] Geophysical Exploration Group, Geophysical Sciences Department, National Research Centre, El-Behoos St., Dokki, Cairo, Egypt
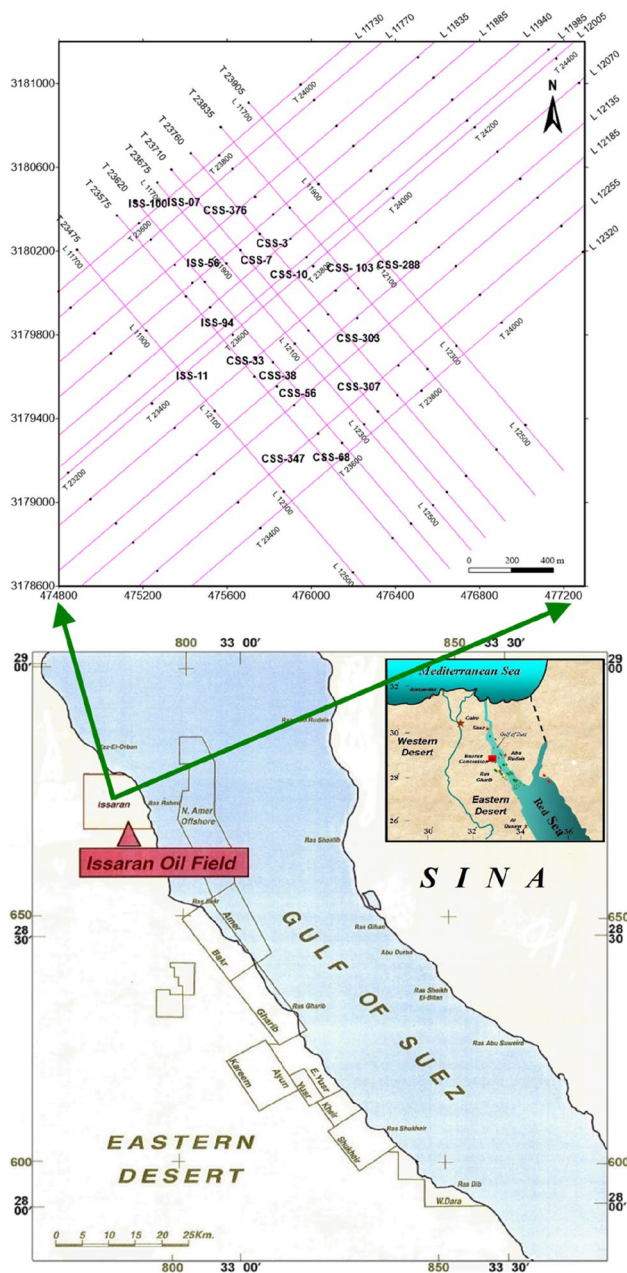
Fig. 1 Location map showing the studied wells and seismic sections, Issaran Field, Gulf of Suez, Egypt

latitudes 28 44′ 4.26"–28 45′ 22.40" N. (Fig. 1). It is roughly 140 km south of Suez City and about 50 km northwest of Ras Gharib Oil Field. The studied region is geomorphologically defined as the clysmic gulf, with slightly NW–SE trending, taphrogenic (rift producing), and regenerated depression (EGPC 1996; Alsharhan 2003). The tectonic history of the Gulf of Suez rift system resulted in the superposition of two distinct sedimentary units: (1) pre-rift sediments (Pre-Miocene) deposited prior to normal block faulting, and (2) syn-rift deposition during rifting. Because of

the presence of reservoir, source, and seal rock, the pre-rift and syn-rift sediments hold the majority of the hydrocarbon accumulations. Syn-rift sediments have been influenced by tectonic forces and exhibit a variety of facies modifications (Khalil and Mesherf 1988).

The present work dealing with evaluation of hydrocarbon potentiality occurred within the facies of depositional environment of the South Gharib Formation that could be differentiated into seven zones of depositional environment. These zones are arranged from base to top as shallow subtidal, shallow lagoonal, intertidal, shallow lagoonal, intertidal, shallow lagoonal and supratidal sabkha cycles, besides the attempts to assess the reservoir petrophysical character, which includes permeability, porosity, and fluid saturations of the southern Issaran Field. The study of core samples from the CSS-38 well, besides the interpretation of Five wire-line logs from the neighboring wells (CSS-288, ISS-100, and CSS-347), and CSS-38 well itself, was used to determine certain petrophysical characteristics. These results may help to explain both the oil recovery and the water production rates.

Geologic setting

Stratigraphy of the study area

The Gulf of Suez rift is divided into three major units that are organized from bottom to top as pre-rift, syn-rift, and post-rift sedimentary periods (Fig. 2). Precambrian basement rocks, Nubia Sandstone, Nezzazat Group (mixed-facies portion), and broad carbonate layer make up the pre-rift sedimentary sequence. This sedimentary sequence ascends stratigraphically as Uppermost Cretaceous chalk, Paleocene shale, and Eocene limestones.

A red-bed clastic part of Abu Zenima Formation (Oligocene–Early Miocene age) covers Miocene sediments with two facies. The first facies is a clastic-dominant section of the Nukhul, Rudeis, and Kareem Formations, and the second is an evaporate-rich layer that is largely anhydrite and salt (Belayim, South Gharib and Zeit formations). Finally, carbonate and clastic sediments are found in post-rift deposits (Abul-Nasr 1990; Garfunkel and Bartov 1977). The Miocene portion covers peripheral facies in the Issaran Field region, which primarily consists of five reservoir zones organized from top to bottom as Zeit sand, South Gharib, two dolomite units (Belayim comparable), Gharandal, and Nukhul Formations. The core investigation reveals that the South Gharib Formation is primarily composed of carbonates with few sulfates, which grade upward into sulfate-rich beds in the upper part, and laminated dolomitic limestone with evaporites, which grades downward into laminated dolomitic limestone and marly limestone in the lower part. In the
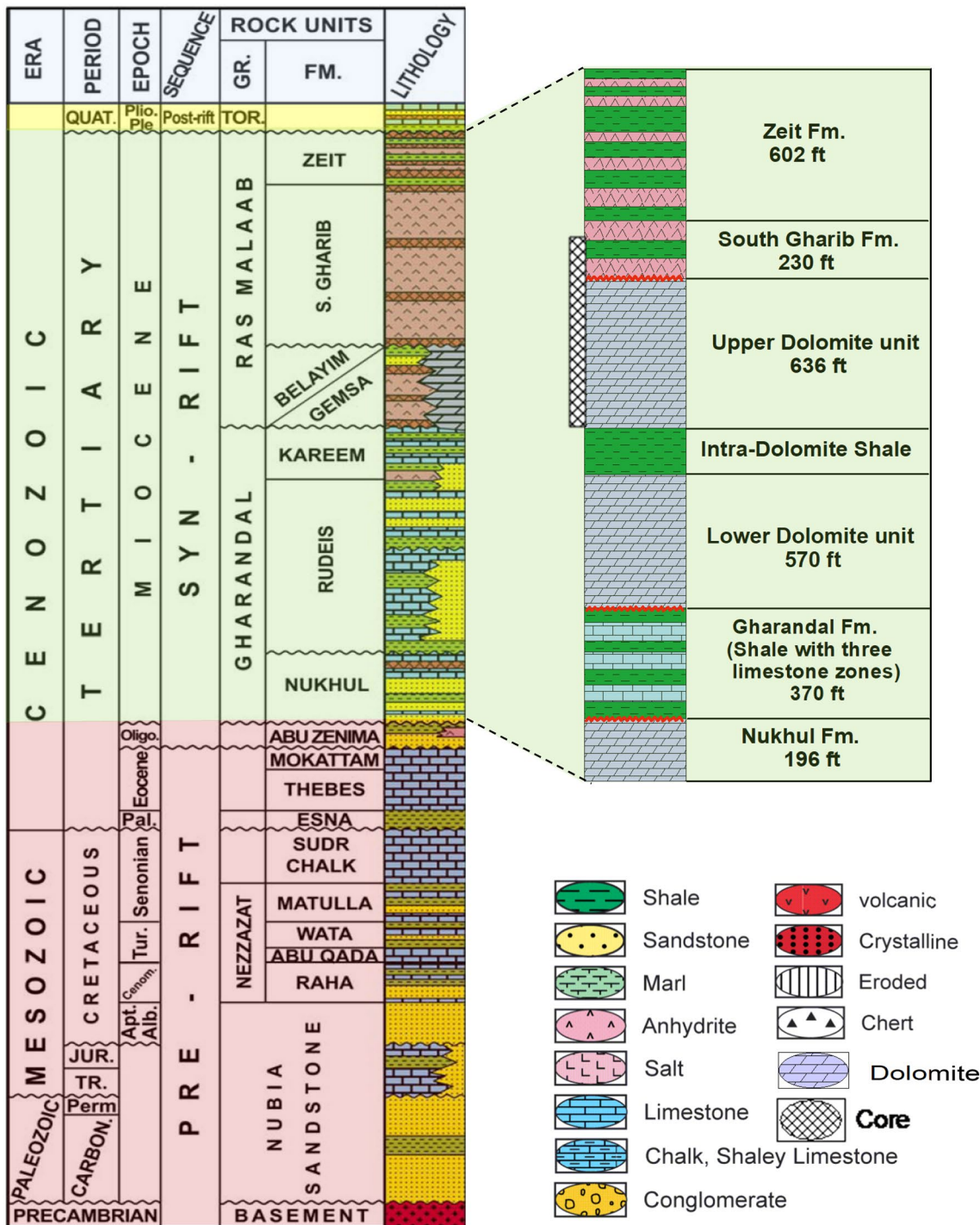
Fig. 2 Simplified stratigraphic section of the Suez rift with detailed Syn-rift Miocene stratigraphic section of the Issaran Field (Modified after Saoudi et al. 2014)

base anhydrite and dolomite units, there is patchy oil staining (Scimictar 2009).The depositional environment of the South Gharib Formation could be differentiated into seven zones. These zones are arranged from base to top as shallow subtidal, shallow lagoonal, intertidal, shallow lagoonal, intertidal, shallow lagoonal and supratidal sabkha cycles. South Gharib Formation rests conformably under the Zeit Formation and unconformably above the top dolomitic rock layer (Fig. 2).

Data sets and methods

The wire-line log data were analyzed using interactive petrophysics software (IP V.3.6) to estimate petrophysical properties, resulting in a wetted average of wells. These wells were contoured and mapped using surfer-8 software. The assembled LAS files raw data of resistivity, neutron, density, gamma ray and caliper logs corrected prior being used to determine lithology, effective porosity, and fluids type saturation of the target zone. Many trials were done to connect the resistivity data of wells to the surface measurements (Gomaa 2022; Gomaa 2021a, b, Gomaa et al. 2021, Ammar et al. 2021). The fundamental parameters that impact the reading and interpretation of logs were used to determine the mud kinds and borehole conditions. This might result in wrong interpretation and misinterpretation of the geophysical records if no action is taken. As a result, before any interpretation is attempted, environmental modifications should be performed or applied to wire-line logs (Cudjoe et al. 2016; Nazeer et al. 2016). Wire-line log files from the CSS-38, CSS-347, ISS-100, and CSS-288 wells were chosen for analysis in the southern Issaran concession compressional block. Wire-line logs and core analyses are primarily used in reservoir appraisal to evaluate effective porosity (ϕ_{eff}), lithology matrix, shale volume (V_{Sh}), hydrocarbon saturation (S_{hc}), and water saturation (S_w). For matrix identification of the South Gharib Formation (Schlumberger 1998), a cross plot of neutron porosity (NPHI) versus bulk density (RHOB) was developed, which relates to predominantly anhydrite and dolomite with minor plotted spots on the cross plot resembling intercalated limestone and shale (Fig. 3). According to Pickett (1973), the formation water resistivity (R_w R_w) may be effectively measured using dual lateral log deep (LLD) against porosity cross plot (0.068 Ohm. m), which was utilized to compute the empirical value of S_{hc} and S_w of the examined interval (Fig. 4). From the (M–N) cross plot, minerals were identified which are primarily reliant on the log parameters and fluid of the examined reservoir, which are effectively merged in the three porosity logs of *sonic* (Δt), density (ρ_b), and neutron (ϕ_N) from these values, two functions M and N may be computed, which are not dependent on primary porosity values (Bruke et al. 1969, Schlumberger chart 1989).

The following formulas are used to compute M and N:

$$M = \left(\Delta t_f - \Delta t / \rho_b - \rho_f\right) \times 0.01, \tag{1}$$

$$N = \phi_{Nf} - \phi_N / \rho_b - \rho_{bf}, \tag{2}$$

where Δt_f is the fluid interval transit time (μs/ft), Δt is the log interval transit time(μs/ft), ρ_b is bulk density of the formation(gm/cc), ρ_f is density of the fluid, (gm/cc), ϕ_{Nf}
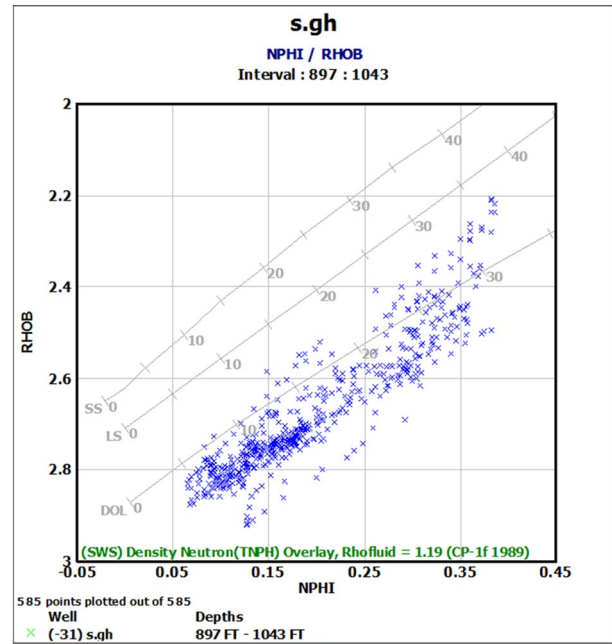

Fig. 3 Neutron–density cross plot for South Gharib Formation, CSS-38 well, Issaran Field, Gulf of Suez, Egypt
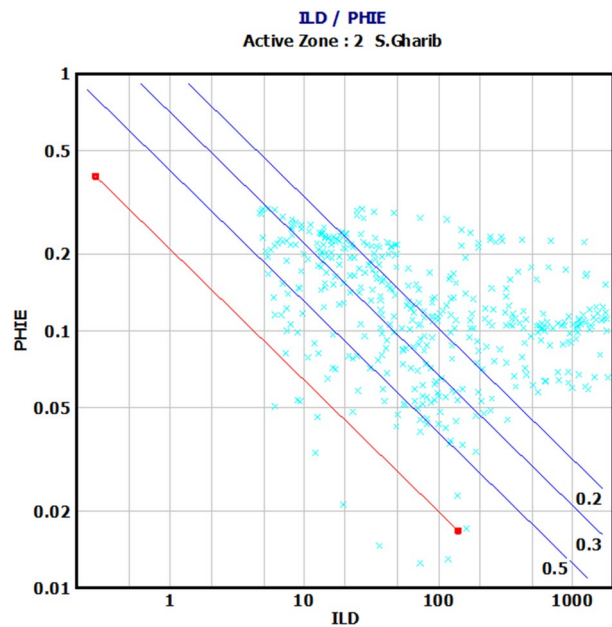

Fig. 4 A Pickettplot for (Rw) determination, South Gharib Formation, CSS-38 well, Issaran Field, Gulf of Suez, Egypt

is the fluid of neutron porosity (P.U) and ϕ_N is the neutron porosity reading (P.U).The examined formations displayed spots on the M–N cross plot approximate anhydrite and dolomite, while a few points correspond to calcite and shale sections. Few displayed dots extend into the secondary porosity region, indicating the impact of diagenetic processes in
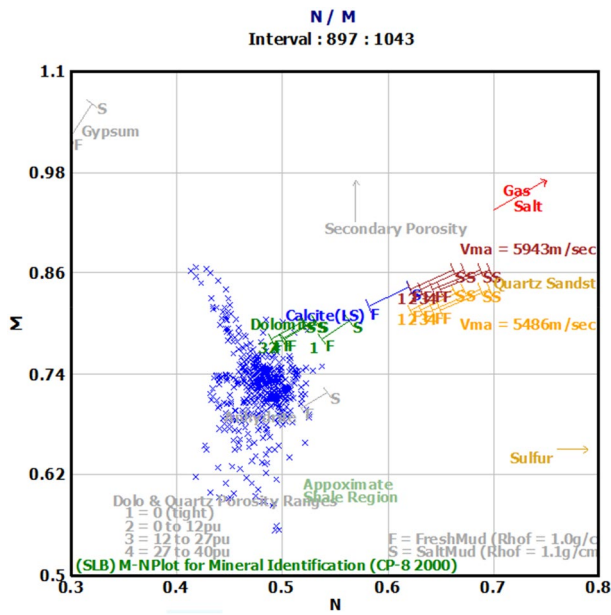
Fig. 5 M–N cross plot for South Gharib Formation, CSS-38 well, Issaran Field, Gulf of Suez, Egypt
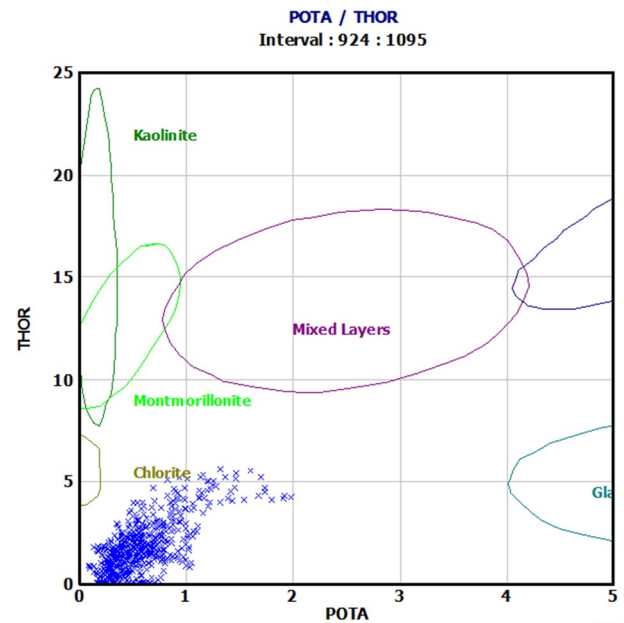

Fig. 6 Potassium–Thorium cross plot for clay mineral identification, South Gharib Formation, CSS-68 well, Issaran Field Gulf of Suez, Egypt

the reservoir (Fig. 5). Furthermore, examinations of a thorium–potassium concentration cross plot (Schlumberger 1984) reveals that all plotted data are around the montmorillonite and chlorite clay minerals regions (Fig. 6). The shale volume is calculated using five log-signature indicators: gamma ray, resistivity, neutron, neutron–resistivity, and neutron–density. The average of these indicators is close to the real value. The Schlumberger equation (1972) is used to calculate corrected effective porosity (ϕ_{eff}) based on the combination of neutron and density logs after different corrections:

$$\phi_{eff} = \frac{2\phi_{NC} + 7\phi_{DC}}{9} \left(1 - 0.10\, S_{hr}\right), \tag{3}$$

where ϕ_{NC} is the corrected neutron porosity; ϕ_{DC} is the corrected density-derived porosity and S_{hr} is the residual hydrocarbon saturation. The Indonesian equation is used to determine and discriminate the fluid contents. The cutoffs used to determine the pay zone are $\phi = 7$ percent, water saturation = 50%, and shale volume = 35%. The petrophysical parameters are displayed vertically by building litho-saturation cross plots that show the overall nature of the petrophysical parameters. These characteristics are also represented laterally by the creation of a set of iso-parametric maps (i.e., iso-shaliness, iso-effective porosity, net-pay thickness, water saturation, and hydrocarbon saturation).
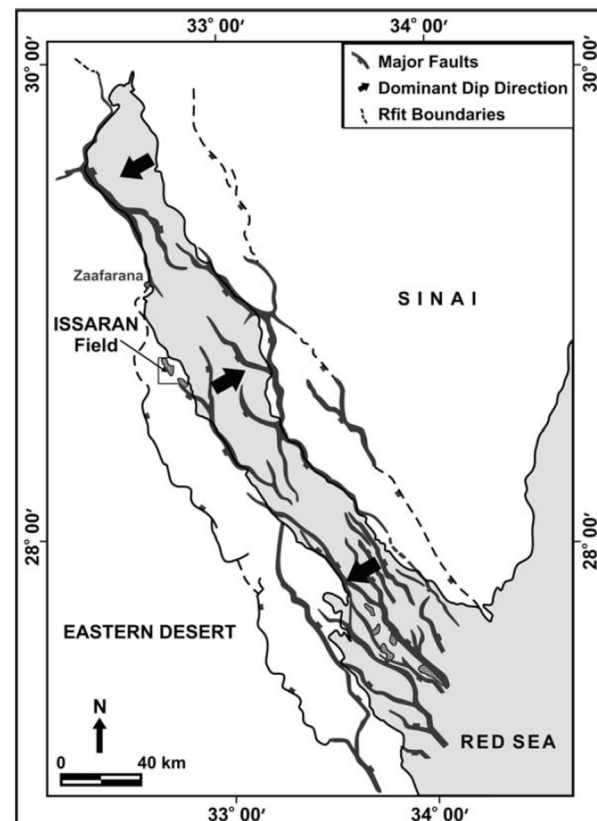

Fig. 7 Structural map of the Gulf of Suez rift showing the location of Issaran Field. Thick arrows refer to dip directions of three provinces (After Patton et al. 1994)
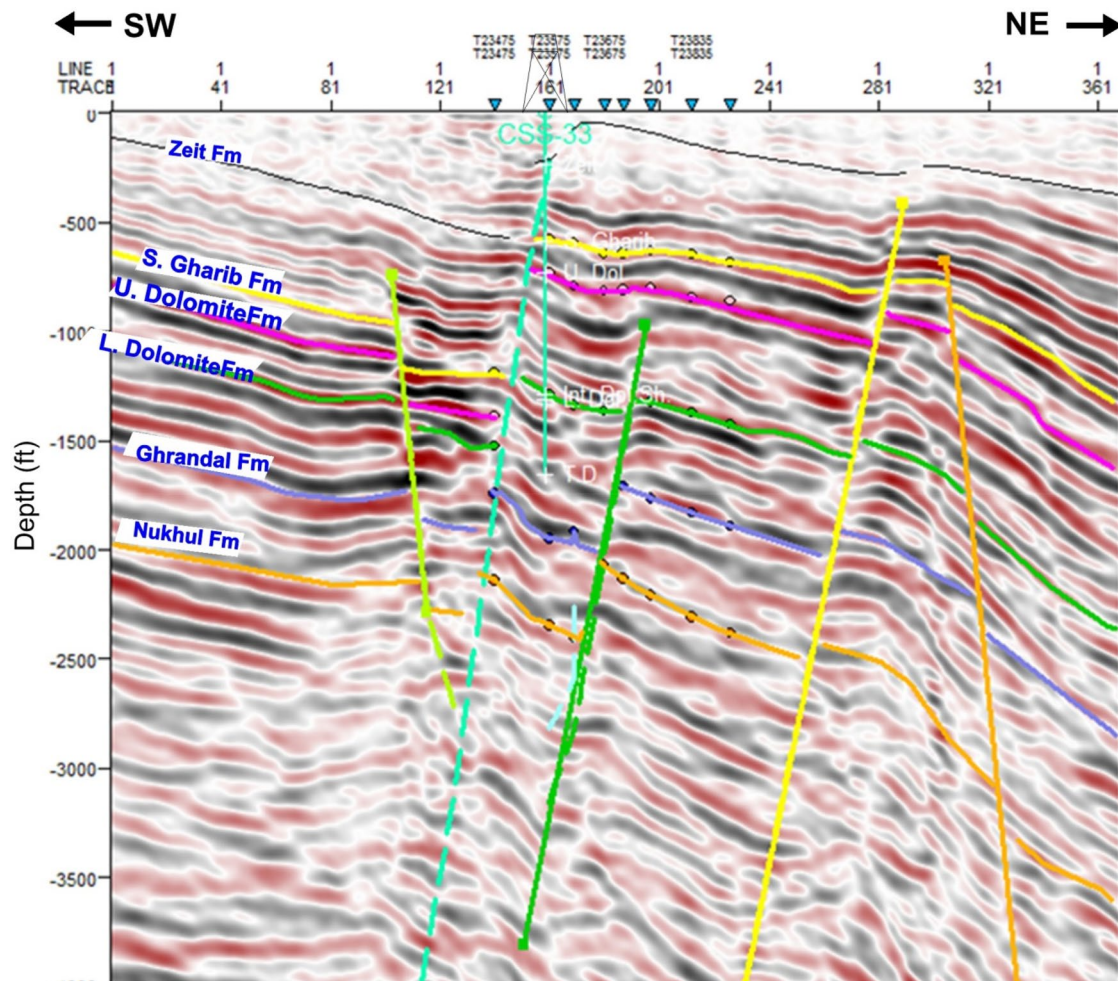
Fig. 8 Interpreted (SW–NE) Seismic line (L 12,070) showing formation tops of the syn-rift Miocene rocks and structural elements in the study area of Issaran oil Field

Structural setting of the Issaran Field

The structural setting of the Gulf of Suez is controlled by two major alignments: the clysmic trend, which is directed northwest–southeast and follows the Gulf of Suez, and the Aqaba trend, which is oriented northeast–southwest and parallels the Gulf of Aqaba (Robson 1971; Khalil and Mesheref 1988; EGPC 1996).The structure of the central province of the Gulf of Suez has a greater impact on the study region, with significant faults dipping toward the southwest SW and strata dipping toward the NE (Fig. 7).It is classified as a tilted fault block with a massive downthrown block to the southwest and a normal fault on the southwest flank. The downthrown normal fault block is often to the southwest and displaces oil–water contacts (EGPC 1996). The region was shaped by a complicated tectonic history and a sequence of extensional releases during the Eocene and Miocene epochs. The area is dominated by fault connection and growth structure occurrences. The fault creates

the lateral principal seals for the trapping of hydrocarbons, and the most productive wells occur inside the field around the faults (Scimitar 2009). The traps found in the research region are classified as stratigraphic, structural, or combination traps (Saoudi et al. 2014). Selected twenty depth-domain seismic lines traversing the research region were chosen to identify features and clarify the structure of whole areas. Along these sections, a collection of normal faults is detected, with structural throws mostly to the SW but a few structures dipping to the NE, forming tilted fault blocks with step-like faults that encircled a small graben. The structural contour map constructed on top of the South Gharib Formation is defined as a tilted fault block. This fault block has a significant downthrown block to the SW that is separated by a NW–SE fault (clysmic trend) in the west and N–S oriented faults generating trap structures in the NE half (Emad 2019; Gomaa and Sedeek 2021; Gomaa et al. 2020; Gomaa 2020 Gomaa et al. 2019). The high structural blocks can be found in the center of the research area between fault 3 (F3) and
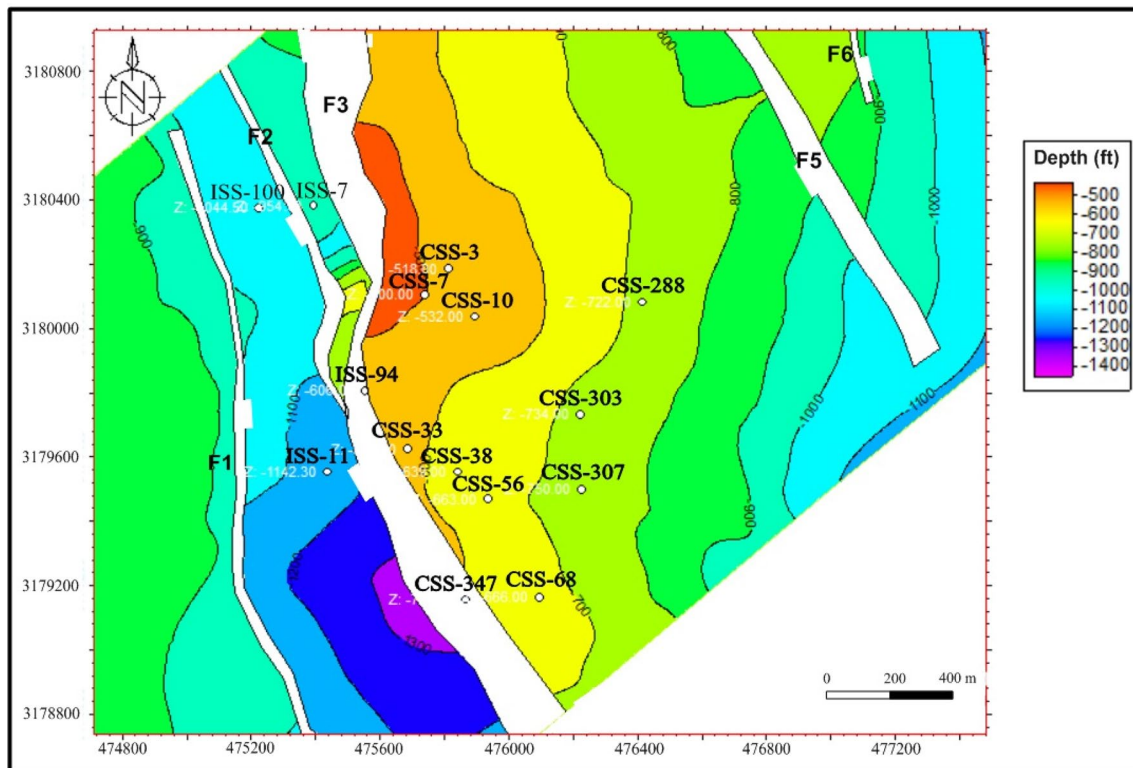
Fig. 9 Depth map drawn on top of the South Gharib Formation, Issaran Field, Western shore of the Gulf of Suez, Egypt, C. I. = 100 ft, (After Emad 2019)

fault 5 (F5), while the low structural region can be found in the southwestern half of the study area between fault 1 (F1) and fault 3 (F3) (Figs. 8, 9).

Discussion and results

The work's findings are mostly based on a petrophysical study of the South Gharib reservoir. This is illustrated vertically by litho-saturation cross plots, which show the overall nature of the analyzed wells' petrophysical properties in terms of porosity, fluid saturation, and lithology fractionation. These data are supported by CSS-38 well core sample analysis (Core No. 1: 960.00'–1021.06' = 61.5 feet, Core No. 2: 1021.06'–1066.00' = 44.5 feet), and represented by literally constructing from a group of iso-parametric maps including iso-shaliness, iso-effective porosity, net-pay thickness, hydrocarbon, and water saturation.

Vertical variation of petrophysical parameters

Litho-saturation cross plots (CPI)

The vertical distribution of the analyzed reservoir's petrophysical properties is illustrated by the production of

numerous litho-saturation cross plots (CPI).The litho-saturation cross plot of the studied wells shows that the shale content of the South Gharib reservoir (Upper Miocene) oscillates by an average amount not exceeding 16 percent along the studied section, and the porosity is not greater than 30 percent with mean values equal to 7 percent in all studied wells. It is obvious from the dramatic rise in resistivity values caused by cementation or compaction in the absence of water content under this situation (Ali et al. 2019).Because of the cyclic steam injection project in this field, water saturation has reached 70% on average. Significant incidences of hydrocarbon saturation (heavy oil) are found along the examined reservoir (Fig. 10).The histograms of core samples from the CSS-38 well show that 20–30% of oil saturation (S_o) is the dominant value with a median value of 22.4 percent and an arithmetical value of 21.8 (Fig. 11A), whereas 7–10% is the common porosity value with a median value of 9 percent and an arithmetical value of 11.7 in the studied reservoir (Fig. 11B).

The laboratory examination of the core samples indicates that the porosities documented in the carbonate layers are mostly of the linked inter-crystalline type, particularly in the dolomitized portions, and predominantly of the unconnected moldic type in beds rich in bioclasts or fossils. Minor unconnected inter-crystalline holes can be seen contained
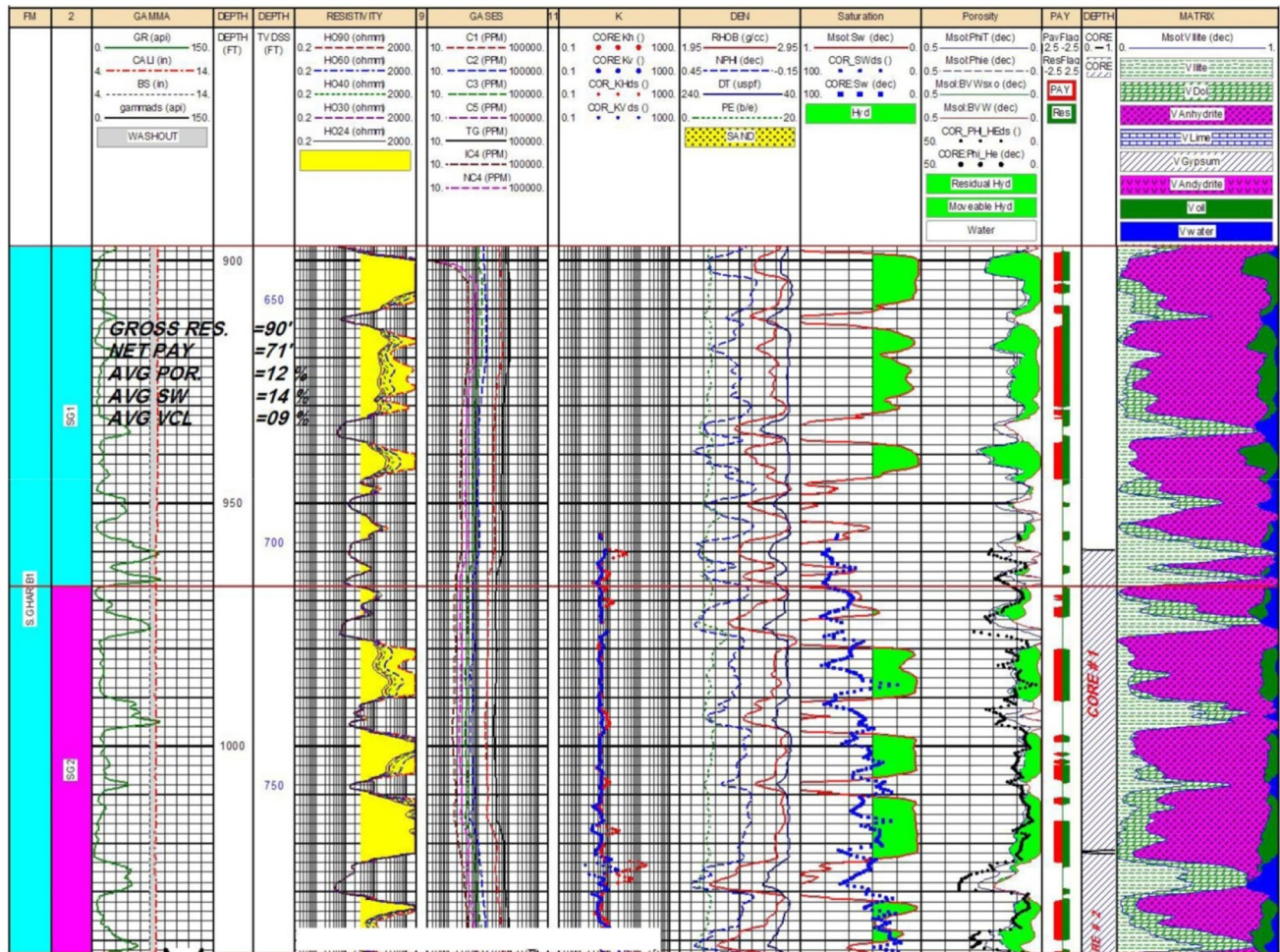
Fig. 10 Litho-saturation cross plot of South Gharib Formation in CSS-38 well, southern Issaran Field, Gulf of Suez, Egypt

between anhydrite or gypsum laths, although significantly more typically linked inter-crystalline pores can be seen in carbonate stringers enclosed between nodules. Minor quantities of fracture porosity are also observed, particularly in dolomite and calcite strata. In the carbonate and evaporitic strata, replacements by secondary fibrous rose gypsum, porphyritic anhydrite, and gypsum blocked the porosity. The laboratory study revealed that there were low to moderate levels of hydrocarbons present (Fig. 12).

Integration of petrophysical parameters

The petrophysical measurement findings of the analyzed core samples are combined to understand reservoir properties, which are graphically depicted shortly below;

– Bulk density (ρ_b) and grain density (ρ_g)

The bulk density of the examined reservoir varied from 2.79 to 3.04 gm/cc, with an average of 2.88 gm/cc, reflecting

the lithology of anhydrite, dolomite, and limestone. The grain density rises as the bulk density rises, until the correlation coefficient between them reaches $r = 0.64$ (Fig. 13).

– Permeability (k)

The permeability is tested in two dimensions in the laboratory to demonstrate the uniformity of the examined reservoir in horizontal and vertical directions. Permeability measurements vary from 1.4 to 84 md in the horizontal direction, with an average of 6.5 md. In the vertical direction, it varies from 0.8 to 54 md, with an average of 4.26 md. For the CSS-38 well, the relation coefficient (r) between horizontal and vertical core permeabilities is 0.65, indicating a heterogeneous reservoir impacted by diagenetic processes. Furthermore, the horizontal permeability to vertical permeability ratios (Permeability Anisotropy; λ_k) are thought to reflect the texture of the rock, with the majority of plotted points being close to laminated rock ($\lambda_k = 1.1$–5), and a few points

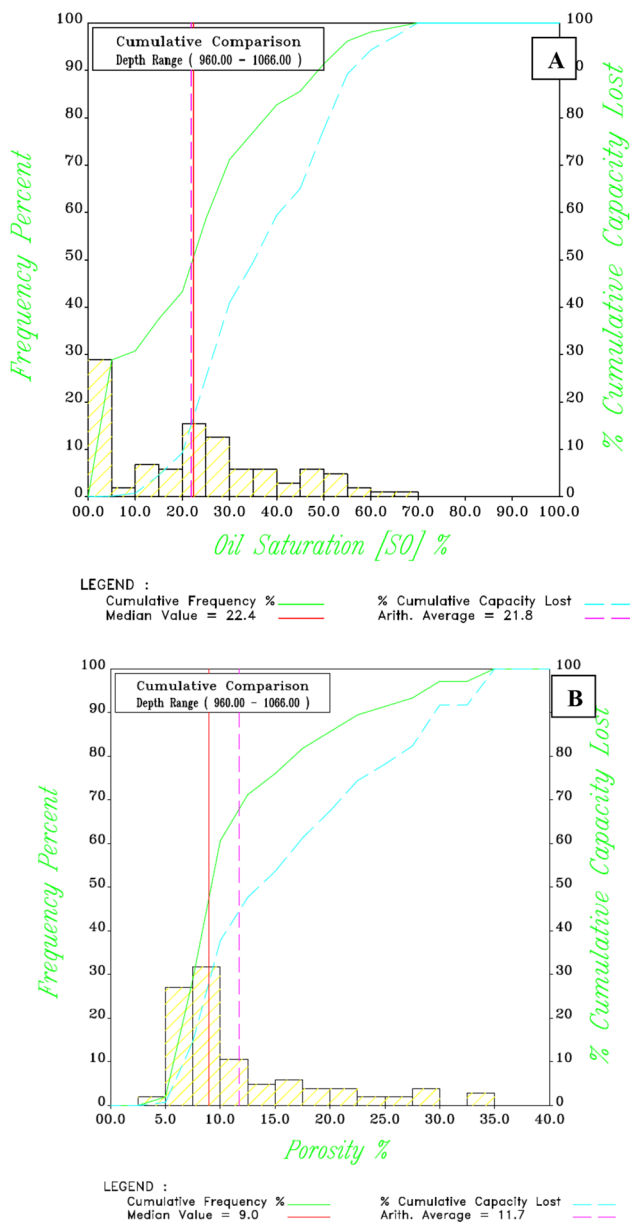**Fig. 11 A** Oil saturation histogram and **B** Porosity saturation histogram of core rock samples of the South Gharib reservoir, CSS-38 well, southern Issaran Field, Gulf of Suez, Egypt

being isotropic ($\lambda_k = 1/1.1$–1.1) and others being fractured ($\lambda_k = 1/2.5$–1/1.1) permeability (Figs. 14).

– Porosity (ϕ) and Permeability (k)

Within the analyzed reservoir samples, the observed helium porosity varied from 3.4 percent to 34 percent with an average value of 11 percent, while the measured fluid porosity ranged from 2 to 37 percent with an average value of 11 percent.

The coefficients (r) relating porosity to permeability in horizontal and vertical dimensions are $r = 47$ and $r = 37$, respectively, indicating that the examined reservoir has been exposed to post-diagenetic processes (Fig. 15).

Lateral variation of petrophysical characteristics

The key elements influencing the lateral distribution of petrophysical parameters in the examined field are thought to be sedimentary facies, diagenetic processes, and structural context (Emad 2019; Emad and Gomaa 2022).The following are the lateral distributions indicated by several sets of iso-parametric maps created for the South Gharib reservoir:

Effective porosity map

The effective porosity map reveals that the values vary from 10.3 percent in the CSS-288 well to 18.7 percent in the CSS-347 well and steadily rise toward the south, indicating that there are no abnormalities in the studied region (Fig. 16A). The primary variables influencing the porosity distribution within the examined reservoir are the sedimentary facies and post-diagenetic processes (Fig. 12).

Iso-shaliness map

The shale volume variation map is an essential indication for assessing reservoir properties in the studied area. The South Gharib reservoir iso-shaliness distribution map revealed that the maximum recorded shale volume is 18.5 percent and 17.6 percent at CSS-347 and ISS-100 wells, respectively, which closed to the lower structure area, and the minimum recorded value is 8.6 percent at CSS-38 wells around the up throw side of the western part of the study area. It is clear that the structural setting has a significant impact on the deposition and dispersion of shale material in the research region (Fig. 16B).

Water-saturation map (S_w)

The water-saturation distribution map indicates a relatively more controlled structural setting, with the maximum S_w value 19.5 percent recorded in the low structure area (ISS-100 well) at depth 1389 feet, and the lowest value 14.3 percent recorded in CSS-38 well at depth 897 feet on the upthrow side. The overall trend of water saturation rises as one moves away from the research region (Fig. 16C).

Hydrocarbon saturation map (S_O)

The hydrocarbon saturation distribution map in the research region varies from 80 to 86 percent. Within varying depths ranging from 897 to 1414 ft., saturations increase toward
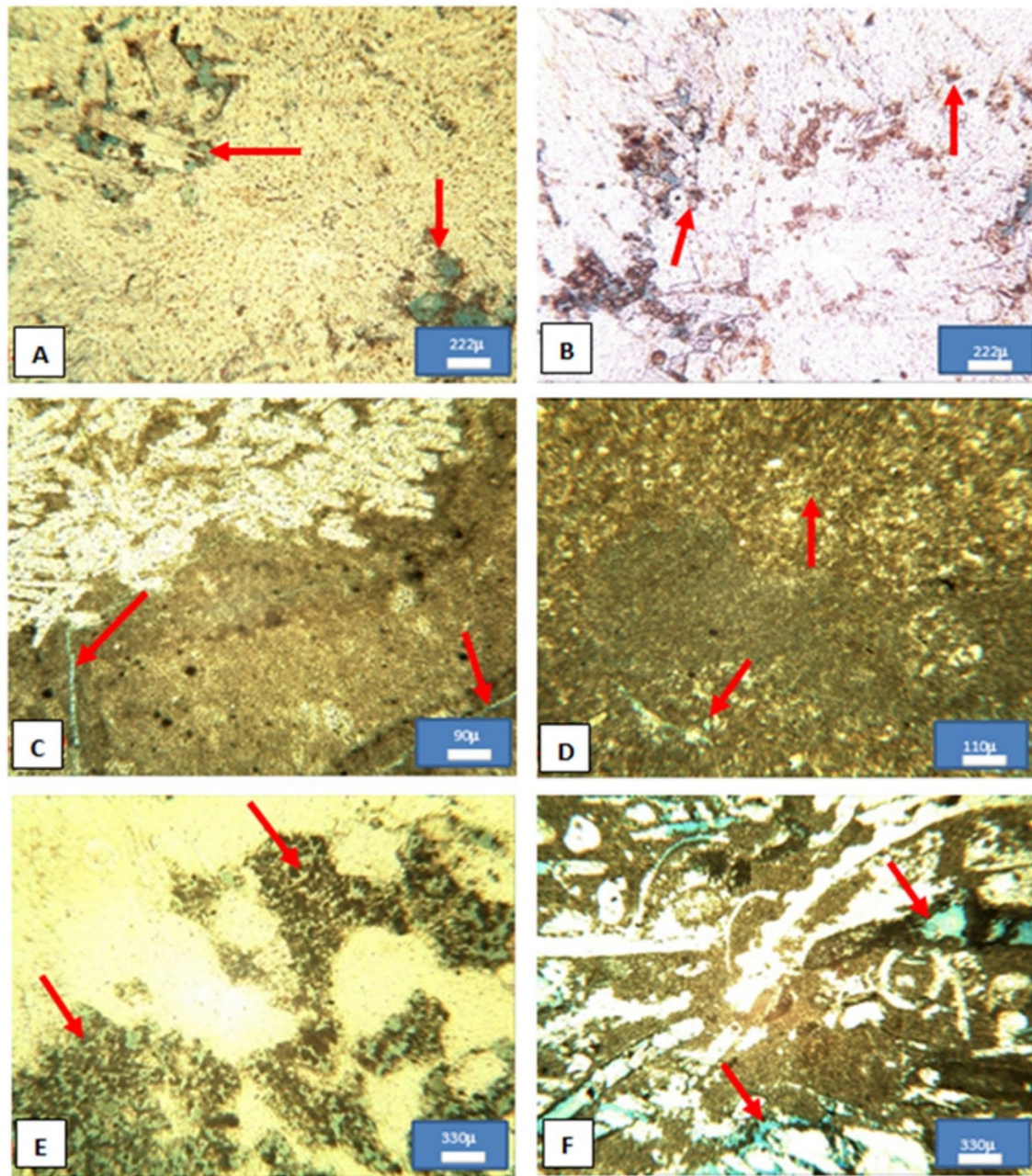
Fig. 12 Porosity types of South Gharib reservoir; **A** Partly connected inter-crystalline, Depth: 1022.07 ft. **B** Disconnected inter-crystalline, Depth: 1026.06 ft. **C** Micro-facture porosity, Depth: 1028.05 ft. **D** Inter-crystalline porosity, Depth: 1031.11 ft. **E** Dissolved pelletal dolomitic L.st. causing connected inter-granular porosity, Depth: 1038.05 ft. **F** Moldic porosity, Depth: 1042.07 ft

the center of the research region and decrease outward (Fig. 16D).Finally, the South Gharib Formation exhibits a large number of pay zone intervals.

The net-pay map

The net-pay thickness distribution map shows that it ranges from 3.9 ft (ISS-100 well) to 71.1 ft (CSS-38 well), with the middle portion of the studied area being the most favorable

for hydrocarbon accumulations, confirming the relationship between hydrocarbon potentiality and the structural setting of the study area (Fig. 16E).

Isochore map of South Gharib reservoir

The isochore map shows that the thickness of the South Gharib Formation gradually from southern parts toward northwestern parts, with no anomalous trend in thickness

Fig. 13 Bulk density–grain density cross plot of the studied South Gharib reservoir, southern Issaran Filed, Gulf of Suez, Egypt
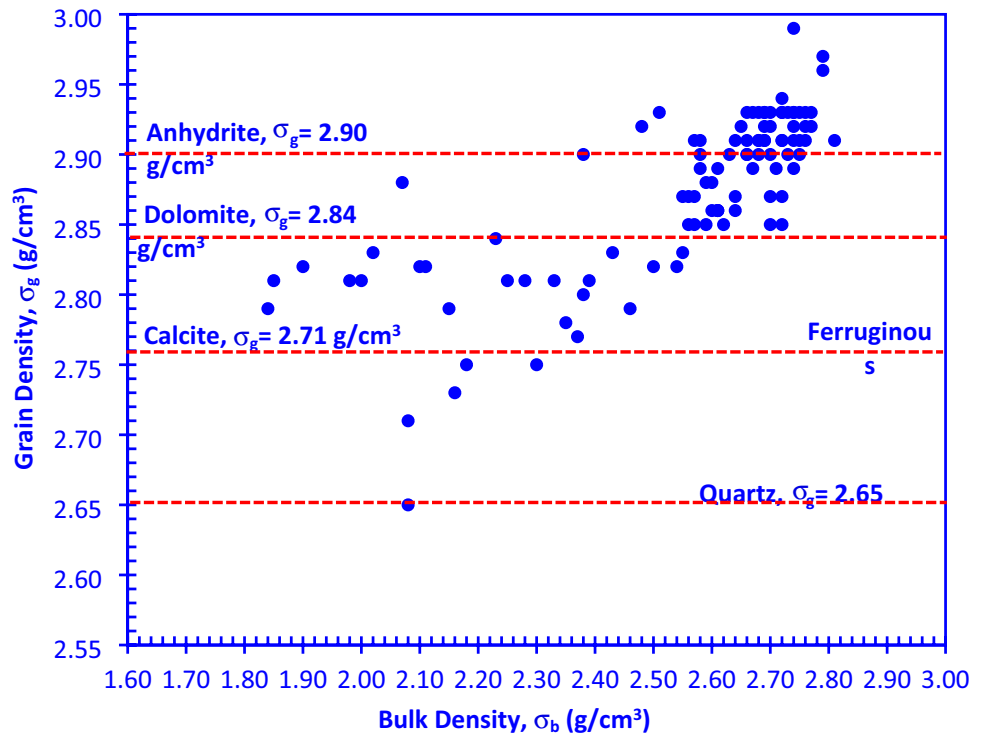
Fig. 14 Horizontal permeability (Kh) versus vertical permeability (Kv) of the South Gharib reservoir, southern Issaran Filed, Gulf of Suez, Egypt
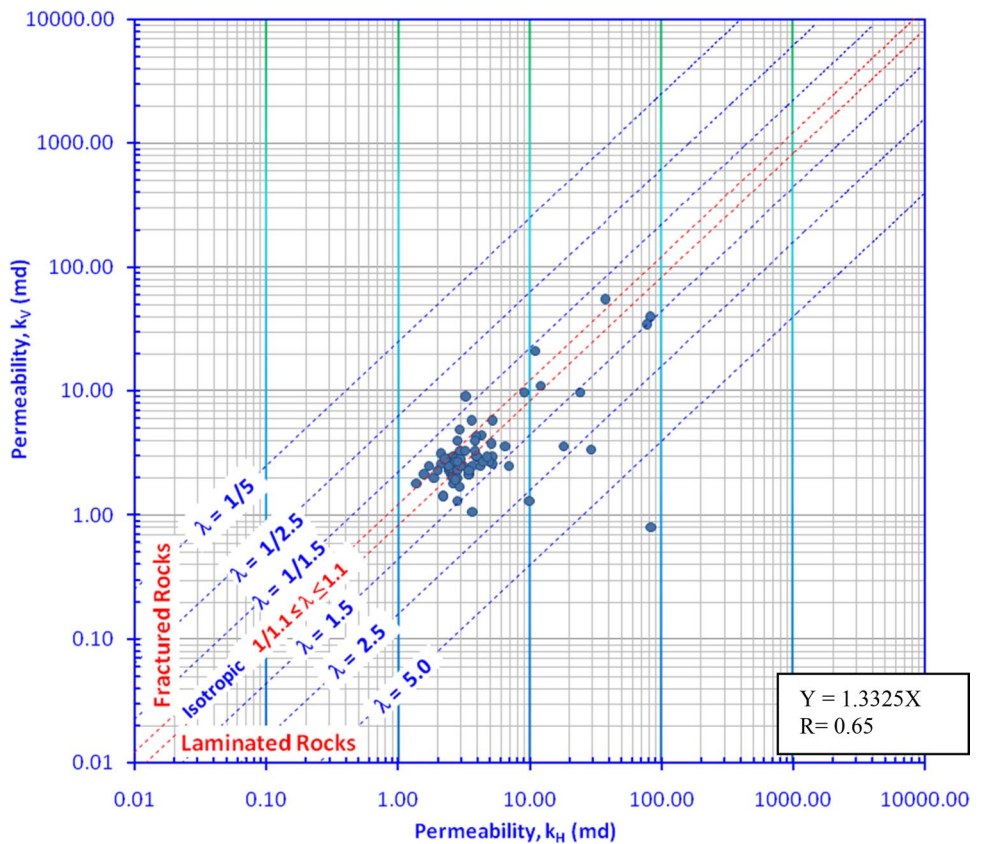
is observed in the studied area, and the depocenter of the studied formation lies in the northwestern part of the study area close to the downthrown side of major faults. Generally, the distribution and deposition of the studied formation
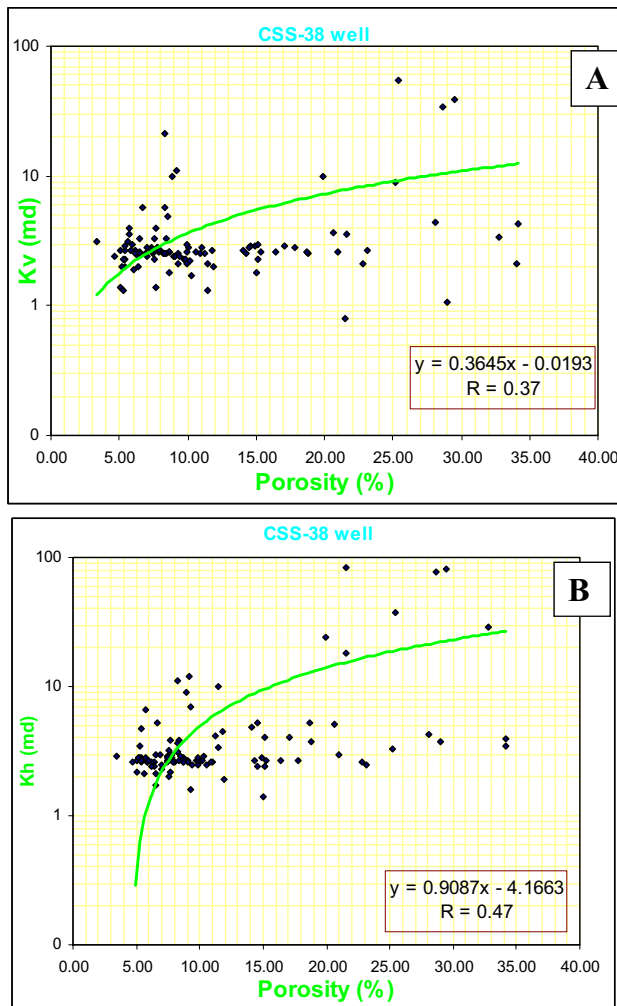
Fig. 15 **A** Porosity versus horizontal permeability Kh and **B** Porosity versus vertical permeability Kv of the studied South Gharib reservoir, southern Issaran Filed, Gulf of Suez, Egypt

are controlled by the structure setting of the study area (Fig. 16F).

Reservoir characters

The reservoir characterization can be accomplished based on different parameters of the conventional core rock including porosity (measured by He and fluid), permeability (kV and kH), density (bulk and grain densities, σb and σg) and water saturation (SW). There are different parameters introduced by many authors to establish the rank of reservoir characterization and discriminate the studied rock sequences into reservoir rock types as Flow Zone Indicator (FZI), Normalized

Fig. 16 Lateral distribution of petrophysical parameters of the South ▶ Gharib Formation in the study area of Issaran Field, **A** Effective porosity distribution map, **B** Shale volume distribution map, **C** Water-saturation distribution map, **D** Hydrocarbon saturation distribution map, **E** Net-pay thickness distribution map and **F** Isochore map of South Gharib Formation, (C. I. = 8ft)

Porosity Index (NPI), Reservoir Quality Index (RQI) (Amaefule et al. 1993).

Reservoir Quality Index (RQI) of the studied reservoir reached to 0.43, Normalized Porosity Index (NPI) reach to 0.52, Reservoir potential index (RPI) reaches to 5.3 and the Flow Zone Indicator (FZI) reach to 10.2 representing good reservoir in many levels. whereas porosity exceed than 25% in many level representing very good to excellent reservoir parameters (Fig. 17).

Conclusion

The depocenter of the investigated formation is located in the western half of the fault, close to the downthrown side. In general, the distribution and deposition of the studied formation continue the structure setting of the study area, where it is described as a tilted fault block with a major down drop or throw to the SW dissected by NW–SE faults (clysmic trend) in the west and N–S oriented faults forming trap structures in the NE part. The South Gharib Formation core sample porosities are classified as linked inter-crystalline, moldic, unconnected inter-crystalline, and fracture porosity. The ratio of horizontal permeability to vertical permeability reflects laminated rock ($\lambda_k = 1.1$–5), with a few points approximating isotropic ($\lambda_k = 1/1.1$–1.1) and fractured porosities ($\lambda_k = 1/2.5$–1/1.1).The coefficients (r) connecting porosity to permeabilities in horizontal and vertical dimensions are $r = 47$ and $r = 37$, respectively, reflecting the post-diagenetic process impacting the examined reservoir. The shale content increases in the western half of the research region, whereas the effective porosity increases in the southern section of the study area. Water saturation increases as one move away from the research area, but net-pay thickness and hydrocarbon saturation are higher at the center of the study area. The middle portion of the study area should be drilled for more hydrocarbon production and economic development of the South Gharib reservoir. Also, more studies about the post-diagenetic process and lateral sedimentary facies change should be applied for the studied field.
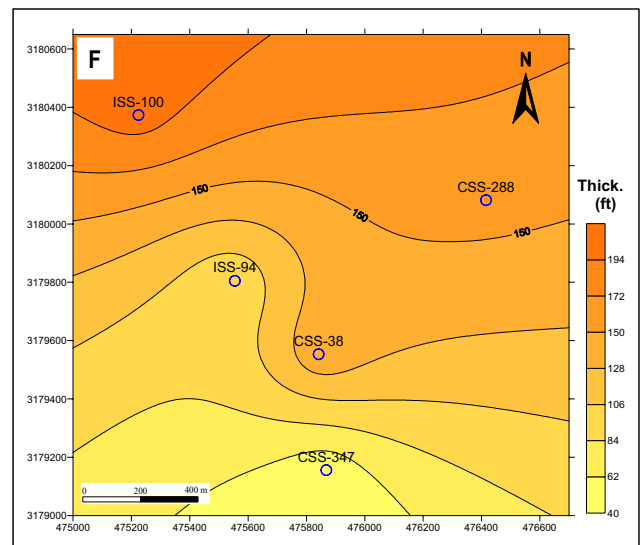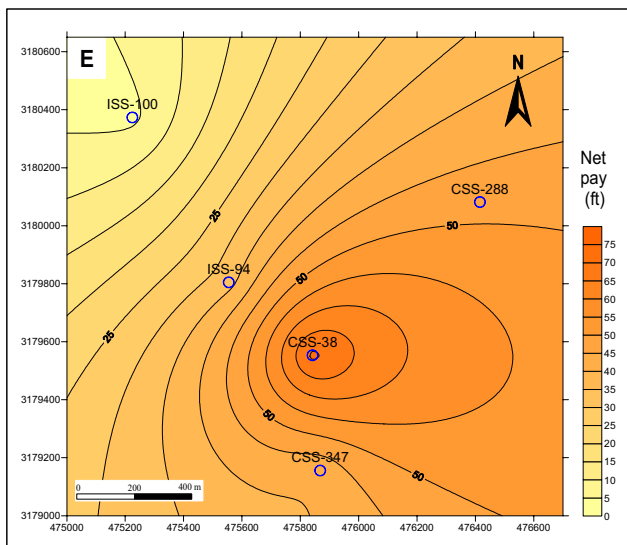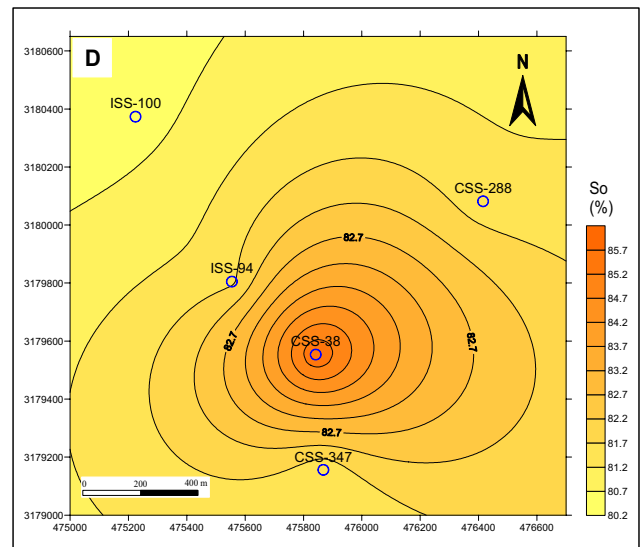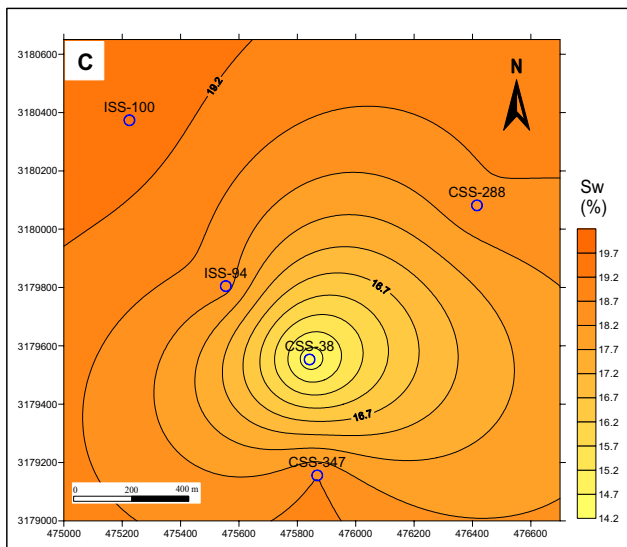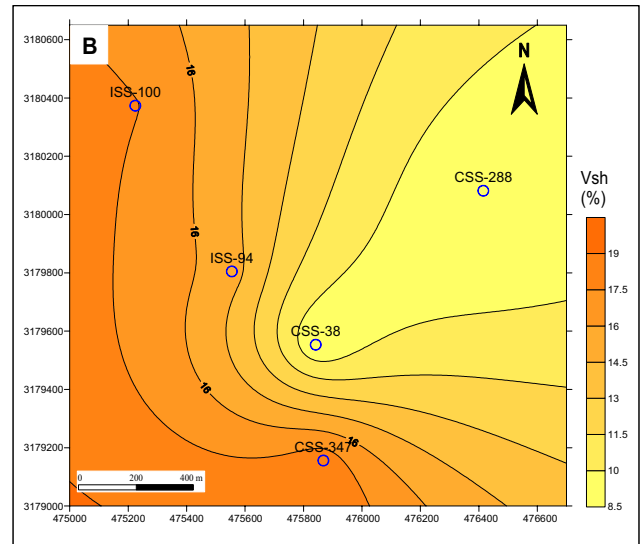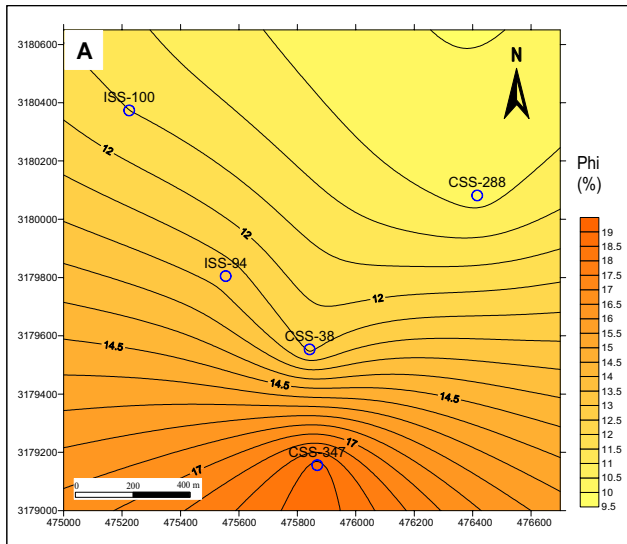
Fig. 17 Vertical reservoir characterization of the South Gharib Formation, Gulf of Seuz, Egypt
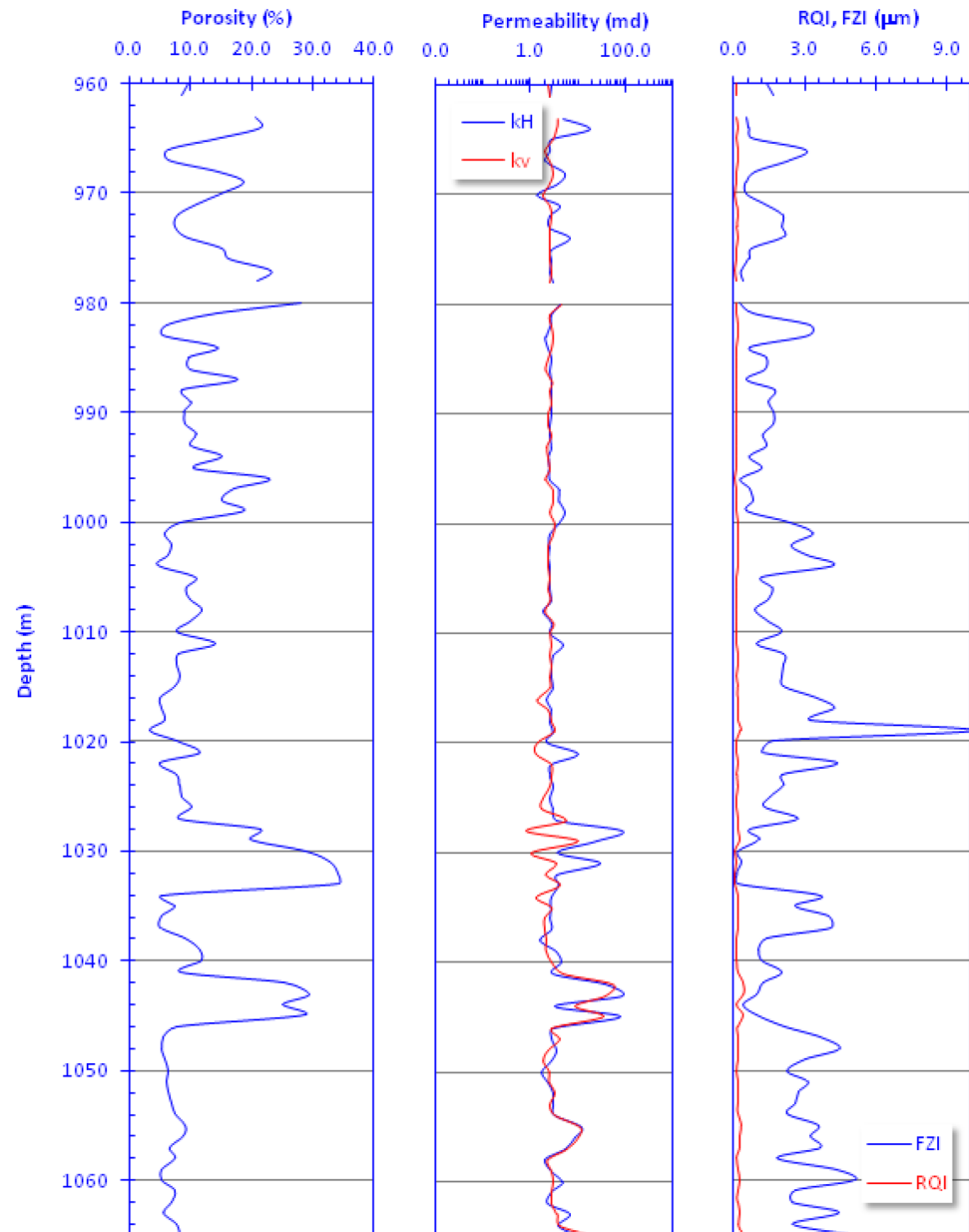
Declarations

Conflict of interest The authors declare that there is no conflict of interest.

References

Abul-Nasr RA (1990) Re-evaluation of the upper eocene rock units in west central Sinai, Egypt Ain Shams Univ, Earth Sci Series 4 234 247

Ali M, Khan MJ, Ali M, Iftikhar S (2019) Petrophysical analysis of well logs for reservoir evaluation: a case study of BKadanwari gas field, middle Indus basin, Pakistan Arab J Geosci 12 215 12

Alsharhan AS (2003) Petroleum geology and potential hydrocarbon plays in the Gulf of Suez rift basin, Egypt AAPG Bull 87 143 180

Amaefule JO et al (1993) Enhanced reservoir description: using core and log data to identify hydraulic (flow) units and predict permeability in uncored intervals/wells. In: SPE annual technical conference and exhibition, Houston, Oct 1993, pp 205–220. https://doi.org/10.2118/26436-MS

Ammar AI, Gomaa MM, Kamal KA (2021) Applying of SP, DC-Resistivity, DC-TDIP and TDEM soundings in high saline coastal aquifer. Heliyon 7(7):1–20. https://doi.org/10.1016/j.heliyon.2021.e07617

Burke JA, Campbell RL, Schmidt AW (1969) The litho-porosity cross plot a method of determining rock characteristics for computation of log data. In: Paper presented at the SPE Illinois Basin Regional Meeting, Evansville, Indiana, Oct 1969. https://doi.org/10.2118/2771-MS

Cudjoe S, Vinassa M, Gomes JH, Barati R (2016) A comprehensive approach to sweet-spot mapping for hydraulic fracturing and CO_2 huff-n-puff injection in chattanooga shale formation. J Nat Gas Sci Eng 33:1201–1218

Emad AA (2019) Seismic and petrophysical analysis for detecting hydrocarbon occurrences of the fractured dolomite reservoir in Issaran Field, Western Shore of the Gulf of Suez, Egypt. Ph.D. Al Azhar University, Cairo, Egypt

Emad AA, Gomaa MM (2022) Electrical properties of sedimentary microfacies and depositional environment deduced from core analysis of the syn-rift sediments, Northwestern shore of Gulf of Seuz, Egypt. J Pet Explor Prod Technol, in print

Egyptian general petroleum corporation (1996). Gulf of Suez oil and gas fields, a comprehensive overview. Cairo, Egypt 520–528

Garfunkel RL, Bartov Y (1977) The tectonic of the suez rift: geological survey of Israel Bulletin 71 1 44

Gomaa MM (2020) Kaolinite under pressure at audio frequency range and its electrical features NRIAG J Astronomy Geophys 9 1 176 189

Gomaa MM (2021a) Grain shape and texture effect on electrical characterization of semi-conductor semi-insulator mixture Arab J Geosci, Special Issue Geol Africa, 9th and 10th Conf, Egypt. https://doi.org/10.1007/s12517-021-08517-x

Gomaa MM (2021b) Using electrical properties of some subsurface sedimentary rocks as a tool to detect bedding direction J Earth Space Phys 46 4 13 26 ISSN: 2538-3906

Gomaa MM (2022) Frequency response of electrical properties of some granite samples physics J Earth Space Phys 47 4 75 86

Gomaa MM, Sedeek H (2021) Prediction of heterogeneity and anisotropy of oxidised pyrite crystals using electrical measurements NRIAG J Astronomy Geophys 10 1 244 257

Gomaa MM, Elnasharty M, Rizzo E (2019) Electrical properties speculation of contamination by water and gasoline on sand and clay composite. Arab J Geosci. https://doi.org/10.1007/s12517-019-4767-4

Gomaa MM, Melegy A, Metwally H, Hassan S (2020) Geochemical and electrical characterization of heavy metals in contaminated soils. Heliyon. https://doi.org/10.1016/j.heliyon.2020.e04954

Gomaa MM, Elshenawy A, Basheer A, Kotb A, Moawad M (2021) Electrical properties of a dry mixture of sand and shale. The 6th Int Conf Eng Geophy, 25–28 Oct 2021, Virtual Conference, Al Ain, UAE, P10, p 299–302. https://doi.org/10.1190/iceg2021-076.1

Khalil B, Mesheref WM (1988) Hydrocarbon occurrences and structural style of the southern Suez rift basin, Egypt 9th Petrol Expl Prod Conf, EGPC Cairo, Egypt 1 86 109

Nazeer A, Abbasi SA, Solangi SH (2016) Sedimentary facies interpretation of gamma ray (GR) log as basic well logs in Central and lower indus basin of Pakistan Geodesy Geodyn 7 432 443 https://doi.org/10.1016/j.geog.2016.06.006

Patton TL, Moustafa AR, Nelson RA, Abdine AS (1994) Tectonic evaluation and structural setting of Gulf of Suez rift SM London Eds Interior rift basin 59 American association of petroleum Geologists USA 9 55

Pickett GR (1973) Pattern recognition as a mean of formation evaluation. Paper A in 14th annual Logging symposium transactions: society of professional well log analysis, paper A 1–21

Robson DA (1971) The structural of the Gulf of Suez clysmic rift with special reference to the Eastern side J Geol Soc 127 247 276

Saoudi A, Moustafa AR, Farag RI, Omara MM, Wally H, Fouad A, Tag A, Ragab RZ. (2014) Dual-porosity fractured miocene syn-rift dolomite reservoir in the Issaran Field (Gulf of Suez, Egypt): a case history of the zonal isolation of highly fractured water carrier bed Geological Society, London, Special Publications, 374, first published on September 5, 2012, doi:https://doi.org/10.1144/SP374.7

Scimitar company, Egypt (2009) Special core analysis study, Issaran Field-Egypt. Internal reports

Schlumberger (1972) Log interpretation, charts. Stumberger limited, New York, NY 10017, USA, p 92

Schlumberger (1984) Log interpretation charts, schlumberger well services, USA, p 285

Schlumberger (1989) Log interpretation principles and applications, p 241

Schlumberger (1998) Schlumberger log interpretation principle-applications. Schlumberger educational services, Houston, Texas, p 222